

Discriminating between Tornadic and Nontornadic Thunderstorms Using Mesoscale Model Output

DAVID J. STENSRUD, JOHN V. CORTINAS JR.,* AND HAROLD E. BROOKS

NOAA/ERL/National Severe Storms Laboratory, Norman, Oklahoma

(Manuscript received 9 July 1996, in final form 31 March 1997)

ABSTRACT

The ability to discriminate between tornadic and nontornadic thunderstorms is investigated using a mesoscale model. Nine severe weather events are simulated: four events are tornadic supercell thunderstorm outbreaks that occur in conjunction with strong large-scale forcing for upward motion, three events are bow-echo outbreaks that also occur in conjunction with strong large-scale forcing for upward motion, and two are isolated tornadic supercell thunderstorms that occur under much weaker large-scale forcing. Examination of the mesoscale model simulations suggests that it is possible to discriminate between tornadic and nontornadic thunderstorms by using the locations of model-produced convective activity and values of convective available potential energy to highlight regions of likely thunderstorm development, and then using the values of storm-relative environmental helicity (SREH) and bulk Richardson number shear (BRNSHR) to indicate whether or not tornadic supercell thunderstorms are likely. Values of SREH greater than $100 \text{ m}^2 \text{ s}^{-2}$ indicate a likelihood that any storms that develop will have a midlevel mesocyclone, values of BRNSHR between 40 and $100 \text{ m}^2 \text{ s}^{-2}$ suggest that low-level mesocyclogenesis is likely, and values of BRNSHR less than $40 \text{ m}^2 \text{ s}^{-2}$ suggest that the thunderstorms will be dominated by outflow. By combining the storm characteristics suggested by these parameters, it is possible to use mesoscale model output to infer the dominant mode of severe convection.

1. Introduction

As better computer resources become available, numerical models with greater spatial and temporal resolution are being used routinely in the operational forecasting environment. Already the Environmental Modeling Center is operating in real time a 29-km mesoscale version of the Eta Model (Black 1994), and many universities are running their own local models in real time and sharing the model output with National Weather Service (NWS) forecasters (Steenburgh and Onton 1996; Colman and Mass 1996). This movement to models with smaller grid spacing is due in part to the success of numerical simulations of mesoscale convective systems (MCSs) that indicate significant improvements in quantitative precipitation forecasts, one of the most difficult forecast problems and one that the modernized NWS intends to improve upon (McPherson 1994). Indeed, mesoscale models are able to simulate many of the features associated with MCSs, including heavier convection along the leading edge of the system, a trail-

ing stratiform rain region, surface mesohighs, mesolows and presquall lows, and rear inflow within the stratiform region (Zhang and Fritsch 1986; Zhang et al. 1989; Zheng et al. 1995). While this new era of modeling brings with it the promise of continued improvements in forecast skill, it is important to realize that numerical models remain only one part of the forecasting process. This is particularly true when attempting to forecast the development and evolution of severe local storms using models that cannot resolve thunderstorms explicitly.

Early research on forecasting severe weather events focused upon synoptic-scale features that were present during severe weather outbreaks (Miller 1972). Composite diagrams of these synoptic-scale "ingredients" necessary for severe convection still are used by weather forecasters to assess the severe weather threat (Johns and Doswell 1992). However, it is clear that an examination of these ingredients is not always sufficient. While July and Johns (1993) show that forecasters from the severe local storms unit of the National Severe Storms Forecast Center have shown considerable skill in forecasting severe weather outbreaks associated with strong large-scale forcing for upward motion (termed synoptically evident outbreaks), Johns and Hart (1993) show that differentiating between outbreaks that produce mostly bow echoes and widespread damaging wind reports, and those that produce mostly supercell thunderstorms (long-lived thunderstorms with midlevel rotation) and tornado reports, is difficult. For example,

* Additional affiliation: Cooperative Institute for Mesoscale Meteorological Studies, Norman, Oklahoma.

Corresponding author address: Dr. David J. Stensrud, NSSL, 1313 Halley Circle, Norman, OK 73069.
E-mail: David.Stensrud@nssl.noaa.gov

while there are some differences in the hodographs of the bow-echo and tornadic supercell events, using hodographs to distinguish between these two types of outbreaks has had mixed results in the operational environment. Although many outbreaks contain a mixture of both severe storm types, knowledge of which type of storm is most likely would be very useful in preparing for warning operations within the NWS and in appropriately alerting the public.

Numerous studies have shown that mesoscale features (convective outflows, low-level jets, jet streaks, etc.) also are important in the generation of severe convection (Maddox et al. 1980; Doswell 1987), and these features have been difficult to predict accurately using the 6- and 12-h output from large-scale models. With the advent of real-time mesoscale modeling, these mesoscale features frequently are seen in the model output. Yet many mesoscale features are short lived by definition and occur over relatively small regions. How is a forecaster to evaluate the evolution of these mesoscale features if they are not detectable from the observations? Which ones are important? Do the parameter evaluation techniques developed through an examination of synoptic-scale observations during large severe weather outbreaks work well using mesoscale model output during localized severe weather events? What are the typical gradients of these parameters? How quickly do they change with time? All these questions will have to be dealt with during each forecast shift when trying to assess the severe weather threat.

A recent study suggests that mesoscale models offer both a tremendous opportunity and a tremendous challenge to the operational forecaster (Cortinas and Stensrud 1995). In this study, the ability of a forecaster to interrogate model output intelligently with respect to the behavior of the parameterization schemes is highlighted as a very important skill, since this ability should allow one to better determine when a forecast is likely to be correct and when it is likely to have errors. However, the event examined by Cortinas and Stensrud (1995) was the 21–23 November 1992 severe weather outbreak over the southeastern United States that was associated with strong synoptic-scale forcing and a well-developed convective line. This event is very different from many of the summertime episodes of localized severe thunderstorms that constitute a more frequent severe weather forecast problem. Research on the examination of mesoscale model output on isolated thunderstorms is limited, since these storms are inherently subgrid-scale phenomena. Would mesoscale model output provide any useful information on the location and initiation time of a single thunderstorm, or even on the likelihood of a thunderstorm developing into a supercell?

One of the problems with using mesoscale model output is that the amount of data produced can be overwhelming. Some method for interpreting the model data must be used to help in the forecast decision process.

Thankfully, along with the many improvements in mesoscale modeling, severe storm research has produced physically based severe weather parameters, such as convective available potential energy (CAPE), storm-relative environmental helicity (SREH) (Davies-Jones et al. 1990), bulk Richardson number (BRN) (Moncrieff and Green 1972), and bulk Richardson number shear (BRNSHR) (Droegemeier et al. 1993), that can be used separately and together to help assess the potential for severe convection. These parameters have been very effective in highlighting areas where *rotating* severe convection occurs (Davies-Jones et al. 1990; Davies and Johns 1993; Johns et al. 1993). Although operational forecasters have found the calculation of these parameters from synoptic-scale model output to be useful at times (Johns et al. 1993), early evidence suggests that the calculation of these parameters from mesoscale model output may be even more helpful (Cortinas and Stensrud 1995). It is hoped that given the additional knowledge of how the mesoscale environment influences the development and evolution of severe convective storms, forecasters can use mesoscale model output as guidance for determining not only where and when severe convection may occur but also the mode of convection. The goals of this study are to assess the ability of a mesoscale model to simulate a variety of severe weather events over the United States and to explore several approaches for using mesoscale model output to provide guidance on the location, timing, and mode of severe weather events. Several of the severe weather episodes chosen are synoptically evident outbreaks, while others are more isolated severe convective events.

2. Model description

The model chosen for use in this study is a hydrostatic version of the Pennsylvania State University–National Center for Atmospheric Research (PSU–NCAR) Mesoscale Model Version 4 (MM4) (Anthes and Warner 1978; Anthes et al. 1987). Because of the variety of physical parameterization schemes that can be used in mesoscale models, it is important to briefly mention the parameterization schemes and model framework that are used for the simulations. These include the following.

Nested grid: A two-way interactive nested grid procedure that allows realistic terrain features is used (Zhang et al. 1986). The coarse grid domain has a horizontal grid spacing of 75 km, while the nested grid domain has a horizontal grid spacing of 25 km. All model simulations have 31 vertical sigma levels with the spacing of sigma levels reduced near the ground surface to better simulate the evolution of the planetary boundary layer. While the horizontal grid locations necessarily vary for many of the simulations, the grid spacings remain the same.

Parameterized convection: An implicit Kain–Fritsch convective parameterization scheme for deep con-

vection (Kain and Fritsch 1990) is used for the nested grid, and an implicit Anthes–Kuo convective parameterization scheme (Anthes et al. 1987) is used for the coarse grid portion of the model domain. The trigger function used is the original one proposed by Fritsch and Chappell (1980). A discussion of the importance of trigger functions is found in Stensrud and Fritsch (1994).

Planetary boundary layer: The model incorporates a modified version of the Blackadar (1976, 1979) high-resolution planetary boundary layer parameterization scheme (Zhang and Anthes 1982; Zhang and Fritsch 1986). A force–restore slab model is used to calculate surface temperature over land (Blackadar 1979; Zhang and Anthes 1982). Cloud cover is parameterized using layer-average values of relative humidity (Benjamin 1983).

Explicit precipitation: An explicit bulk microphysics scheme is used with predictive equations for cloud and rainwater below the freezing level, and cloud ice and snow above the freezing level. This scheme is based on the studies of Lin et al. (1983), Rutledge and Hobbs (1983), and Hsie et al. (1984) and includes the effects of hydrostatic water loading, condensation, evaporation, melting, freezing, deposition, and sublimation (Zhang 1989).

Model initialization: The model simulations are initialized by blending the National Centers for Environmental Prediction global analysis data with surface and rawinsonde data using the approach of Benjamin and Seaman (1985). These blended analyses also are used to provide the model boundary conditions. Only one simulation is produced for each severe convective event, and all simulations use the identical physical packages. Results presented focus entirely upon the evolution of the nested grid domain and no information from the coarse grid domain is presented.

Further details of the model can be found in Stensrud and Fritsch (1994), while a detailed description of why we prefer some parameterizations over others is found in Cortinas and Stensrud (1995).

3. Severe weather parameters

Convective available potential energy is defined as the positive buoyant energy available to a parcel as it rises from its initial vertical level upward through the depth of a cloud:

$$\text{CAPE} = g \int_{\text{LFC}}^{\text{ETL}} \frac{\theta(z) - \bar{\theta}(z)}{\bar{\theta}(z)} dz, \quad (1)$$

where $\theta(z)$ is the potential temperature of the parcel as it ascends moist adiabatically through the cloud, $\bar{\theta}(z)$ is the potential temperature of the environment, g is the acceleration due to gravity, LFC is the level of free convection of the parcel, and ETL is the equilibrium temperature level of the parcel. In the model calcula-

tions, 50-mb layer-average parcels are calculated throughout the first 250 mb above the model surface, and the most unstable parcel is used to calculate the CAPE at each grid point.

The bulk Richardson number is used to quantify the relationship between buoyant energy and vertical wind shear (Moncrieff and Green 1972), such that

$$\text{BRN} = \frac{\text{CAPE}}{0.5(\bar{u}^2 + \bar{v}^2)}, \quad (2)$$

where \bar{u} and \bar{v} are the wind components of the difference between the density-weighted mean winds over the lowest 6000 m and the lowest 500 m above ground level. As discussed in Droegemeier et al. (1993), the BRN is only a gross estimate of the effects of vertical wind shear on convective storms, since it does not measure the turning of the wind profile with height. However, Weisman and Klemp (1984) show using cloud-scale model simulations that the BRN can distinguish between supercell and multicell storms, with modeled supercells likely when $10 \leq \text{BRN} \leq 50$ and multicell storms likely when $\text{BRN} > 35$. It is important to note that there is no well-defined threshold value for BRN, since there is an overlap in these values used to specify storm type.

Storm-relative environmental helicity has been used to forecast the rotational characteristics of thunderstorms by Davies-Jones et al. (1990) and is defined as

$$\text{SREH} = \int_0^h \mathbf{k} \cdot (\mathbf{V} - \mathbf{c}) \times \frac{\partial \mathbf{V}}{\partial z} dz, \quad (3)$$

where h is an assumed inflow depth (frequently chosen as 3000 m), \mathbf{c} is the storm motion vector, $\mathbf{V}(z)$ is the environmental wind profile, and \mathbf{k} is the unit vector in the vertical. Using cloud model simulations, Droegemeier et al. (1993) show that SREH is superior to BRN in predicting net updraft rotation. Thus, they suggest that BRN should be used to predict storm type, since it is independent of storm motion, and that SREH be used to describe the likely rotational properties of storms once their motion is known. Typically, values of $\text{SREH} > 100 \text{ m}^2 \text{ s}^{-2}$ are found in regions where supercell thunderstorms develop, that is, in regions where thunderstorms have a midlevel mesocyclone (Davies-Jones et al. 1990; Moller et al. 1994). Admittedly, this value of $100 \text{ m}^2 \text{ s}^{-2}$ for SREH is low and may lead to the overforecasting of supercell thunderstorm development. While there is some evidence of an increasing likelihood of supercells as the value of SREH increases, there have been no studies examining the occurrences of nonsupercell thunderstorms in environments with SREH greater than $100 \text{ m}^2 \text{ s}^{-2}$. Thus, the best that can be said is that a SREH value of $100 \text{ m}^2 \text{ s}^{-2}$ can be used to indicate regions of *possible supercells*.

In this study, since the mesoscale model is not capable of resolving individual storms, the storm motions are determined using the climatological mean storm motions estimated by Davies and Johns (1993). Thus, the

mean storm motion is defined as 30° to the right of the mean wind and 75% of the mean wind speed if the cloud layer mean wind is less than 15 m s^{-1} , or as 20° to the right of the mean wind and 80% of the mean wind speed otherwise. The cloud-layer mean wind is estimated using the model density-weighted mean wind from 850 to 300 mb.

BRNSHR is defined by the denominator of Eq. (2) and has been found to be highly correlated with the maximum vertical vorticity of modeled thunderstorms by Droegemeier et al. (1993), despite the fact that it does not account for the turning of the wind vector with height or the magnitude of the low-level storm-relative winds (Lazarus and Droegemeier 1990). However, our results suggest it may have another use as well. Brooks et al. (1994a,b) hypothesize that the midlevel, storm-relative winds are important to the development of low-level rotation in thunderstorms. Since their conceptual model indicates that the strength and lifetime of low-level mesocyclones is a function of the balance between low-level baroclinic generation of vorticity and outflow development, they examined the redistribution of rain in modeled supercells. Results indicate that for very weak midlevel storm-relative winds, the low-level mesocyclones are short lived, occur early in the storm life cycle, and low-level outflow dominates the storm. Storms forming in this type of environment are more likely to evolve into squall lines owing to the strong organizing influence of the outflow. For very strong storm-relative winds, low-level mesocyclones develop very slowly, or do not develop at all, and outflow is weak, since the rain is being blown away from the storm by the strong midlevel winds. In the middle of these two extremes, the results of Brooks et al. (1994a,b) show that low-level mesocyclones tend to be long lived, owing to the balance between the mesocyclone circulation and the storm-relative winds.

These results are related to the values of BRNSHR, since an examination of the supercell thunderstorm proximity sounding dataset from Brooks et al. (1994b) indicates that the BRNSHR can be used as a proxy for the storm-relative wind. The use of BRNSHR instead of the storm-relative wind is a valuable simplification, since BRNSHR is both independent of storm motion and vertically integrated, making BRNSHR values better behaved than values of storm-relative midlevel winds calculated from mesoscale model output where the storm motion must be estimated. In addition, using the proximity dataset of Brooks et al. (1994b)¹ and subjectively determining the best fit line to discriminate between tornadic and nontornadic thunderstorms using only the values of SREH and BRNSHR, we find that

¹ Five supercell cases with SREH values less than $100 \text{ m}^2 \text{ s}^{-2}$ have been removed from this proximity dataset since these do not fit the existing paradigm of supercell formation. The remaining dataset contains a total of 65 supercell events.

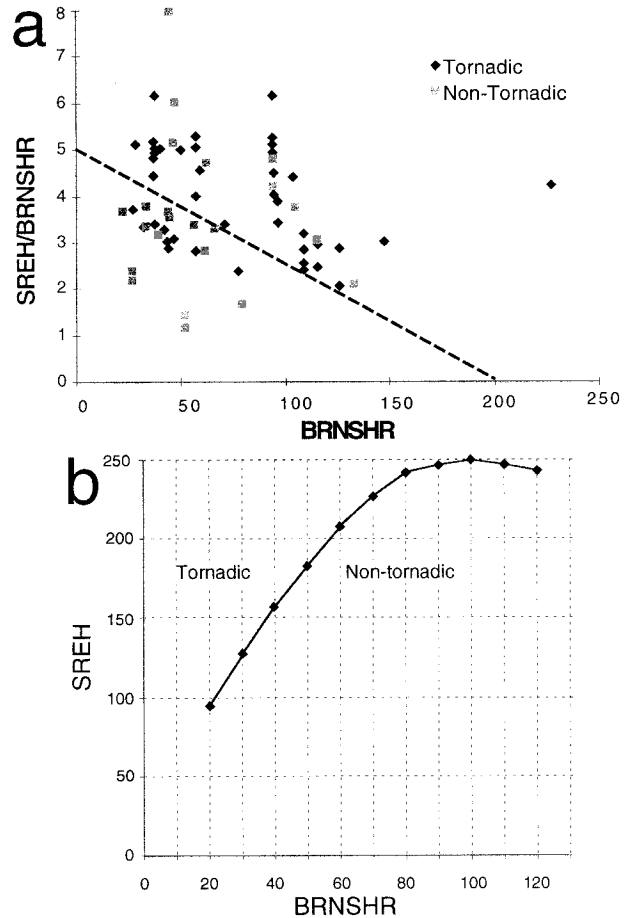


FIG. 1. The (a) SREH/BRNSHR vs BRNSHR ($\text{m}^2 \text{ s}^{-2}$) for proximity soundings using the dataset of Brooks et al. (1994b) where the dashed line indicates the best-fit line to discriminate between tornadic and nontornadic thunderstorms. Summary measures of the skill of the tornadic/nontornadic forecast include probability of detection = 0.79, false alarm ratio = 0.21, critical success index = 0.65, and Heidke skill score = 0.39. (b) The SREH ($\text{m}^2 \text{ s}^{-2}$) vs BRNSHR ($\text{m}^2 \text{ s}^{-2}$) relationship calculated from the best-fit line in (a).

as the value of BRNSHR increases the value of SREH also must increase to support mesocyclogenesis (Fig. 1). No observed tornadic storms occur with BRNSHR values less than $20 \text{ m}^2 \text{ s}^{-2}$ and, except for one outlier, for BRNSHR values greater than $140 \text{ m}^2 \text{ s}^{-2}$. Thus, in more highly sheared environments we expect that the value of SREH must be significantly higher than the guidance value of $100 \text{ m}^2 \text{ s}^{-2}$ in order to increase the likelihood of developing tornadic supercell thunderstorms. This behavior also is consistent with the cloud-scale model simulations conducted by Droegemeier et al. (1993), although the sum total of all the numerical cloud-scale model simulations reported in the literature fail to span the space of the observations very well, leaving large gaps in our knowledge of storm behavior in different environments.

We find that small values of BRNSHR correspond to low values of midlevel storm-relative winds and storms

that are outflow dominated with a tendency to produce damaging winds. This interpretation also is consistent with the results of Weisman (1993), who examined bow echoes using a cloud-scale model. His results show that bow echoes are more prevalent for lower values of BRNSHR, while supercells are more prevalent for larger values of BRNSHR, assuming that there is sufficient shear to generate long-lived rotating storms. For the largest values of BRNSHR used, the results of Weisman (1993) indicate that no organized convective activity occurred in the numerical simulations. Thus, in general agreement with our conceptual model, his results show that it is in the middle range of BRNSHR values that supercell thunderstorms develop. The mesoscale model results, discussed more fully in later sections, suggest that values of BRNSHR between 40 and 100 $m^2 s^{-2}$ indicate a greater likelihood of tornadic supercell thunderstorms if the SREH values are large enough to produce rotating storms. The value of 40 $m^2 s^{-2}$ used for the modeled BRNSHR threshold is larger than that suggested by the proximity sounding data, likely owing to the difficulties in simulating low-level winds.

Before proceeding with an analysis of the mesoscale model output, a few of the challenges in using these parameters need to be highlighted. First, the values of BRN quoted in the literature most often are in reference to numerically simulated storms (Weisman and Klemp 1982, 1984; Droegemeier et al. 1993). How well these values correspond to the real atmosphere and to numerical simulations using mesoscale models is uncertain. In addition, the range of CAPE used in these cloud model simulations is between 1500 and 4000 $m^2 s^{-2}$, yet thunderstorms do occur in lower and higher CAPE environments (Johns et al. 1993; Korotky et al. 1993). In particular, when CAPE approaches 4000 $m^2 s^{-2}$, the BRN calculation begins to lose its usefulness, since the numerator becomes so big that it dominates the calculation and the BRN values are large regardless of the BRNSHR value. For example, assuming a CAPE of 5000 $m^2 s^{-2}$, in order to get BRN=10 the BRNSHR must equal 500 $m^2 s^{-2}$, or the difference in *mean density-weighted winds* over the surface to 500 and the surface to 6000 m levels must be over 31 $m s^{-1}$. This type of strongly sheared wind profile is difficult to create, especially in the types of environments where such high CAPE values are most likely to occur. Also, although BRNSHR and SREH are measures of the vertical wind profile, they can vary in the opposite directions. It is not unusual for BRNSHR to decrease as SREH increases, as can occur with the development of a low-level jet.

To evaluate the importance of these parameters for determining the likely mode of convection, hourly output from nine mesoscale model simulations have been examined (Table 1). In general, the model simulations produce parameterized convection in regions very close, in both space and time, to the observed locations of convection, and the large-scale features evolve similar

TABLE 1. List of cases simulated by the mesoscale model, indicating the time and date of the model simulation, the number of hours simulated, and the general observed characteristics of the convection.

Initialization time (UTC)	Simulation time (h)	Type of event
1200 21 Nov 1992	24	Tornadic supercell thunderstorm outbreak
1200 28 Mar 1984	24	Tornadic supercell thunderstorm outbreak
1200 26 Apr 1991	24	Tornadic supercell thunderstorm outbreak
1200 16 Jun 1992	24	Tornadic supercell thunderstorm outbreak
1200 17 Jun 1992	24	Bow echoes with widespread straight-line wind damage
1200 09 Apr 1991	24	Bow echoes with widespread straight-line wind damage
0000 02 Jul 1992	24	Bow echoes with widespread straight-line wind damage
1200 28 Aug 1990	12	Isolated violent tornadic supercell thunderstorm
1200 27 May 1985	24	Isolated tornadic supercell thunderstorm

to that suggested by observations (except where explicitly noted). Therefore, we assume that the model produces a reasonable representation of the environments in which these thunderstorms developed. Admittedly, it is possible to have what appears to be good simulations for the wrong reasons (Molinari and Dudek 1992). The lack of observations with sufficient temporal and spatial resolution to validate many of the numerical model results leads us to view our conceptual model with some degree of skepticism, and only through repeated operational testing will we be able to evaluate the utility of this conceptual model.

The results presented in this paper are largely based upon calculations from the mesoscale model output, and, therefore, the guidance values for BRNSHR noted in this paper may not correspond exactly to what one would get from observations or another numerical model. For example, the mean value of BRNSHR calculated from the 134 available rawinsonde observations during all nine simulations is 52, whereas the mean value calculated from the model at the same locations is 34. Thus, the model values of BRNSHR are in the mean 66% of the magnitude of the observed values, even though the two datasets have a correlation coefficient of 0.8. This result highlights the difficulties involved in simulating low-level winds accurately. Thus, we suggest caution when using any of our guidance values until one has experience with the model or observational data that is being used to make the calculations. Our analysis has incorporated explicitly any bias in the MM4 values of BRNSHR. The bias of another numerical model likely will be different and result in a slightly different range for the BRNSHR values needed to create low-level mesocyclogenesis.

Of the four parameters examined, our results suggest that the fields of BRN and CAPE convey essentially the

same information. In all the synoptically evident outbreak cases the BRN fields only serve to highlight regions with instability; we can discern no relationship between the model-produced values of BRN and thunderstorm type as described by Weisman and Klemp (1982, 1984) in their cloud-scale modeling study. Since the values of BRN are not useful in high CAPE environments, which occur in some of the cases selected, we have chosen to use CAPE fields instead of BRN fields in the discussion below.

We also must emphasize that we do not expect the model to be able to place parameterized convection exactly where it is observed but instead to place parameterized convection within approximately 100 km of the observed reports. This is because the simulation of convection is an incredibly difficult problem for any model, including those with much smaller grid spacings and nonhydrostatic numerics, and forecasters likely can never expect perfect guidance on convective events. The question we ask is more focused upon whether the models can provide good guidance on the general areas of convective activity and, hopefully, the convective mode. In addition, even though the mesoscale model produces parameterized convection in locations that are often representative of the observations, we advise using the model convective precipitation fields with great care. Although the results from this study suggest that mesoscale models with an appropriate "trigger function" can produce a reasonable evolution of convection (Kain and Fritsch 1992; Stensrud and Fritsch 1994), there are times when the model simulations fail in this regard. Thus, in the discussion below we not only use the locations of model-produced convection to highlight regions of likely thunderstorm development but examine the values of CAPE as well. In this approach one evaluates more of the complete region in which thunderstorms may develop, thus hopefully avoiding any surprise situations when the model convective forecast is poor. Other parameters, such as convective inhibition, may help refine this region and thus avoid the overforecasting that would occur if this approach is used exactly as discussed in this paper (Johns and Doswell 1992). With these caveats to interpreting the model output in mind, we proceed to an evaluation of the mesoscale model runs.

4. Synoptically evident outbreaks of tornadic supercell thunderstorms

a. 21 November 1992

One of the more devastating severe weather outbreaks of 1992 occurred between 21 and 23 November in the southeastern United States. Beginning near Houston, Texas, around 1800 UTC 21 November and continuing into eastern Alabama by 1200 UTC the following day, a swath of tornado reports are found. Over this 2-day event there are 146 reports of tornadoes, 27 of which

are F2 or greater, and 92 reports of severe convective winds. While Cortinas and Stensrud (1995) illustrate that CAPE and SREH values are helpful in locating regions where severe convection is expected, this synoptically evident outbreak is an example of an event that, while well forecast, is difficult to distinguish operationally from one in which damaging straight-line winds are the primary severe weather hazard (see Johns and Hart 1993).

Instability is present only along the gulf coast early at 1800 UTC, while 12 h later the strong southerly flow ahead of the developing cyclone has brought in substantial amounts of warm, moist, low-level air northward through Mississippi and into Tennessee, thereby destabilizing inland areas considerably (Fig. 2). At 1800 UTC, the values of SREH along the Texas coast near where the model produces convection indicate that any long-lived storms that develop are likely to rotate, while a large gradient in values of BRNSHR from 20 to over $150 \text{ m}^2 \text{ s}^{-2}$ indicates that a range of storm behavior is possible, including supercells with low-level mesocyclones. As the convection ahead of the cold front moves eastward over the next 12 h, it enters the region with SREH values above $200 \text{ m}^2 \text{ s}^{-2}$ and BRNSHR values between 40 and $100 \text{ m}^2 \text{ s}^{-2}$, indicating that the storms that form in this environment are likely to develop a balance between baroclinic generation and outflow, indicating that low-level, tornadic mesocyclones are possible. This picture of the most likely thunderstorm evolution agrees well with the observations during this 18-h period, including the observed distribution of BRNSHR values at 0000 UTC. Even the placement of model-produced convection at 1800 and 0600 UTC the following day agrees reasonably well with the observed locations of severe reports (Fig. 2c), including the locations of reported tornadoes at the south end of the model-produced convective line.²

b. 28 March 1984

A major tornado outbreak occurred in the Carolinas on 28 March 1984 associated with the explosive intensification of a continental cyclone (Gyakum and Barker 1988). Damage reports indicate that 7 F4 tornadoes, 5 F3 tornadoes, and 10 tornadoes of F2 or F1 intensity occurred (Fujita and Steigler 1985). This event begins as thunderstorms initiate in northern Alabama and Georgia by 1500 UTC 28 March ahead of a surface front extending southward from a strong low pressure center in Tennessee. The surface low intensifies rapidly over the next 12 h, and the convection is nearly collocated

² The observed convection occurred over a larger area than suggested by the severe reports, such that the model simulation of convective activity at this time is fairly realistic when compared to the national radar summaries. One should not base an assessment of the model convective simulation on the severe reports only.

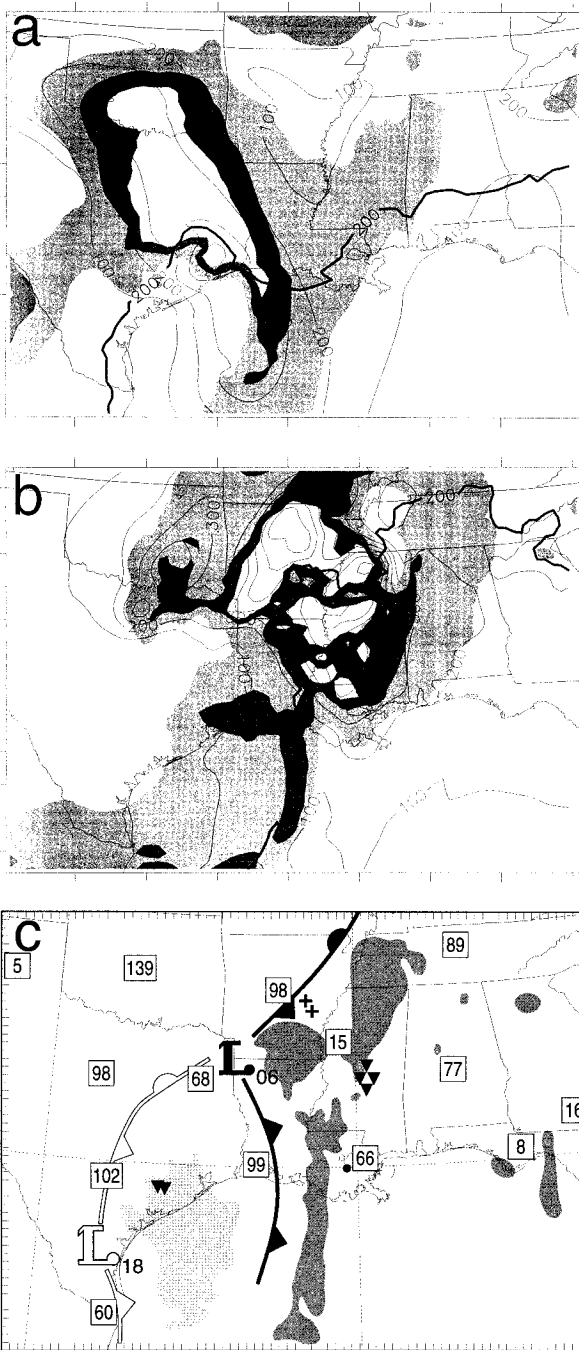


FIG. 2. Fields of BRNSHR ($m^2 s^{-2}$), SREH ($m^2 s^{-2}$), and CAPE ($m^2 s^{-2}$) from (a) 1800 UTC 21 November and (b) 0600 UTC 22 November 1992 produced by the mesoscale model. Thick solid line indicates where CAPE is $200 m^2 s^{-2}$, with higher CAPE values located to the south where simulated convection occurs. Values of SREH contoured every $100 m^2 s^{-2}$ starting at $100 m^2 s^{-2}$, while values of BRNSHR shaded between 40 and $100 m^2 s^{-2}$ (darker shading for values between 70 and $100 m^2 s^{-2}$). Locations of the frontal positions simulated by the model are shown in (c) along with regions of convective rainfall exceeding 1 mm during the past hour valid at 1800 UTC (light shading) and 0600 UTC (dark shading). Times (UTC) of the frontal positions denoted as subscripts on the low center identifier, with earlier time outlined and later time solid. Severe weather shown with a + indicating a severe wind report, a dot indicating a hail

with the surface cyclone during its most rapid intensification (Gyakum and Barker 1988). The strong to violent tornadoes occur in South and North Carolina beginning at 2100 UTC.

The modeled convective rainfall fields closely parallel the observed locations of the severe storm reports, indicating that the model evolution of convection is reasonable (not shown). In addition, values of CAPE are greater than $200 m^2 s^{-2}$ throughout the regions of tornado reports at 0000 UTC (Fig. 3), SREH values are above $200 m^2 s^{-2}$ over a large region, and a narrow zone of BRNSHR values between 40 and $100 m^2 s^{-2}$ is seen stretching from South Carolina into central North Carolina. This narrow zone of larger BRNSHR values is located between two regions of model-produced convection (Fig. 3c), whereas 6 h earlier, prior to convective development, the BRNSHR values ranged from 40 to $100 m^2 s^{-2}$ over much of this same region (Fig. 3a). This reduction in the BRNSHR likely is due to the mixing effects of the convective scheme as discussed in Cortinas and Stensrud (1995) and are not representative of the environment prior to convective development. Thus, even though the region with BRNSHR values expected for low-level mesocyclogenesis is narrow, the evolution of the field suggests that the main cause of the downward trend is the mixing effects of the convective scheme and, therefore, mesocyclogenesis in this region is still considered likely.

The values of BRNSHR over northern Georgia and western South Carolina are above $100 m^2 s^{-2}$ at 1800 UTC (Fig. 3a), which from the conceptual model suggests that any low-level mesocyclones will be unlikely to develop. Thunderstorms formed in this region, as indicated in both the modeled rainfall fields and observations, and produced reports of a few weak tornadoes (F0), hail, and wind damage. In contrast, the model output suggests that low-level mesocyclogenesis is possible in far northeastern Alabama, where thunderstorms developed but only severe wind reports are indicated. While the sparsity of upper-air observations in both time and space make an assessment of the model evolution of BRNSHR difficult (see Fig. 3c), the model results support the notion that BRNSHR values exceeding $100 m^2 s^{-2}$ are too large to allow much outflow to form, and, therefore, low-level mesocyclogenesis is either going to take a long time to develop or not occur at all (Brooks et al. 1994b).

The evolution of these model parameters at a grid point in South Carolina, south of the observed tornado path, indicates that CAPE values do not exceed $700 m^2$

report, and an inverted triangle indicating a tornado report. Severe weather reports from 1800 to 2000 UTC are located in Texas, with reports from 0500 to 0600 UTC located elsewhere. Observed values of BRNSHR at 0000 UTC are denoted within the boxes at upper-air sounding sites. Tick marks in (c) indicate locations of model grid points.

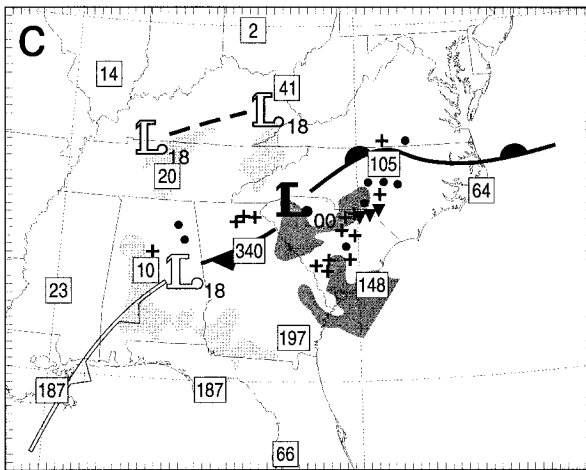
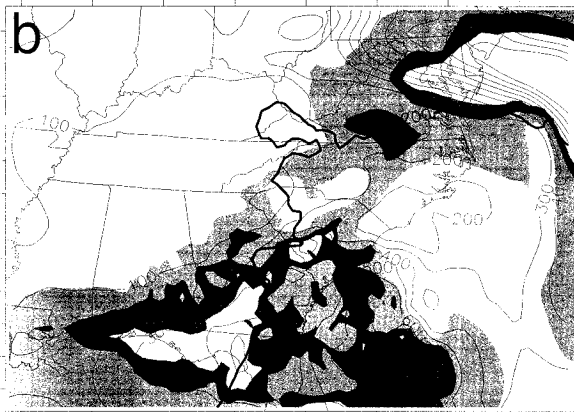
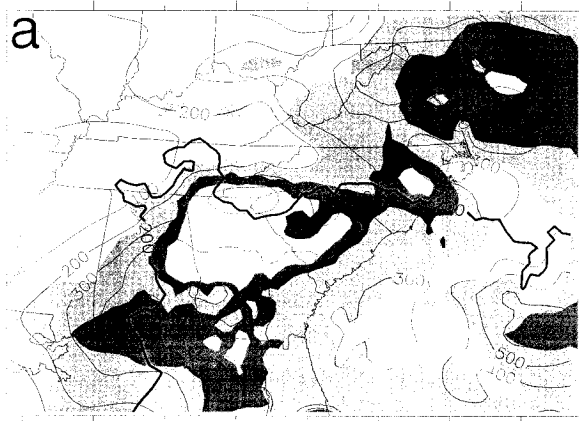


FIG. 3. As in Fig. 2 except from (a) 1800 UTC 28 March, (b) 0000 UTC 29 March 1984, and (c) summary of modeled convection during the preceding hour valid at both times and corresponding severe weather reports. Reports in (c) from the hour preceding 1800 UTC are located in Alabama and Georgia, with reports during the hour preceding 0000 UTC located elsewhere. Large solid dot in South Carolina in (a) denotes location of gridpoint output shown in Fig. 4.

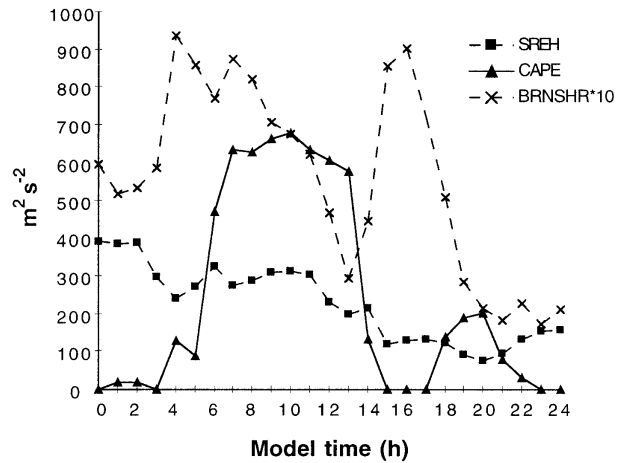


FIG. 4. Plot of values of CAPE ($\text{m}^2 \text{s}^{-2}$), SREH ($\text{m}^2 \text{s}^{-2}$), and BRNSHR ($\text{m}^2 \text{s}^{-2}$) vs model time (h) from a grid point located in South Carolina from the mesoscale model (large solid dot in Fig. 3a).

s^{-2} throughout the entire simulation (Fig. 4). Again, the important information comes from the locations of model-produced convection and the values of BRNSHR and SREH that indicate both the likelihood of rotating storms and the development of low-level mesocyclones. Also important to note is the rapid increase in CAPE from 100 to nearly $500 \text{ m}^2 \text{ s}^{-2}$ over a 1-h period. This indicates that hourly model output is necessary to monitor rapidly evolving environments, along with all available observations.

c. 26 April 1991

Johns and Hart (1993) also chose 26 April 1991 as one of their cases in which it is difficult to distinguish between days with predominantly supercells and tornado reports and days with predominantly bow echoes and damaging wind reports. Of their cases, 26 April is closest to a classic major tornado outbreak in that a number of isolated supercells produced tornadoes over a large region. Fifty-four tornadoes are reported, with 29 rated as F2 or greater, while there are only 66 damaging wind reports. The strong and violent tornado reports (F2 or greater) occur from eastern Texas northward to Iowa, with most of the tornado reports located in eastern Kansas.

At 1200 UTC 26 April, a center of low pressure is present in southwestern Nebraska with a dryline extending southward from the low across western Kansas and into the Oklahoma and Texas panhandles. The dryline pushes eastward rapidly after sunrise and is into western Oklahoma by 1500 UTC. The first storms develop along the dryline after 1800 UTC and evolve into classic supercell thunderstorms.

The mesoscale model reproduces many of these features, including the development of convection after 1800 UTC along the dryline. Values of CAPE at 1800 and 0000 UTC indicate that sufficient instability is pres-

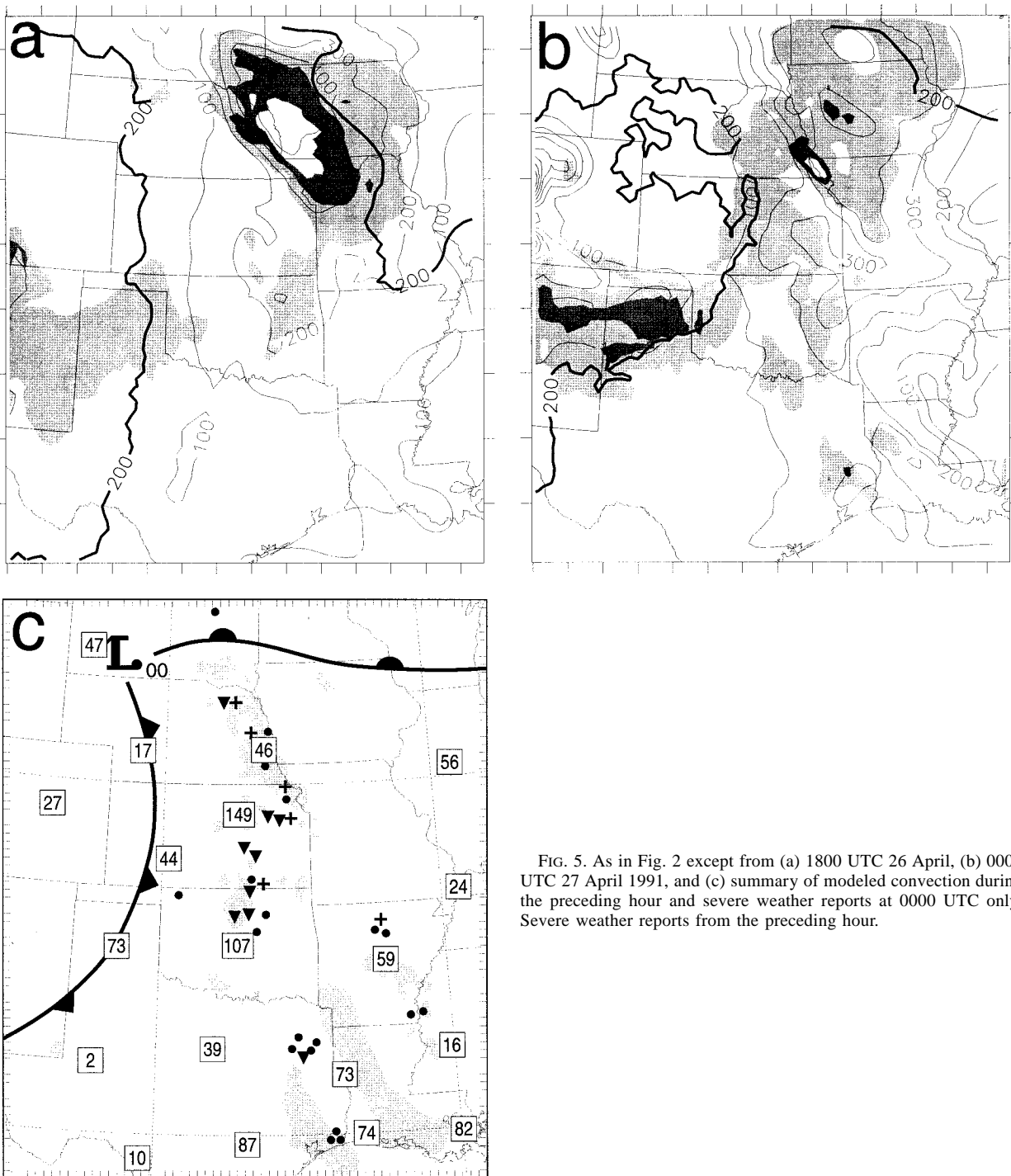


FIG. 5. As in Fig. 2 except from (a) 1800 UTC 26 April, (b) 0000 UTC 27 April 1991, and (c) summary of modeled convection during the preceding hour and severe weather reports at 0000 UTC only. Severe weather reports from the preceding hour.

ent for thunderstorms to develop (Fig. 5). In addition, SREH values are above $200 \text{ m}^2 \text{ s}^{-2}$ indicating that the thunderstorms are likely to rotate, and BRNSHR values are between 40 and $70 \text{ m}^2 \text{ s}^{-2}$ over a broad region ahead of the cold front, suggesting that low-level mesocyclogenesis is possible as well. The modeled placement of convection, overlapping the regions of high SREH val-

ues and moderate BRNSHR values, agrees reasonably well with the observed storm reports indicating tornadic development from Nebraska to southern Kansas. While the tornadoes reported in northern Oklahoma are in a region with BRNSHR values between 30 and $40 \text{ m}^2 \text{ s}^{-2}$ at this time, the values of BRNSHR in this area were greater than $40 \text{ m}^2 \text{ s}^{-2}$ during the previous hour, high-

lighting the need for frequent model output and corresponding observations. Note that the model also reproduced the gap in convective activity from central Oklahoma to northeastern Texas (Fig. 5c).

d. 16 June 1992

During the 14-h period from 1200 UTC 16 June through 0200 UTC 17 June a total of 45 tornadoes were reported (22 rated as F2 or greater) along with 39 damaging wind events (Johns and Hart 1993). The day began with a weak low pressure center located in northwestern Kansas with an associated warm front extending from the low center eastward across northern Kansas and into Missouri. As the day progressed, the low center deepened by 8 mb and moved northeastward into far southeastern South Dakota by 0000 UTC 17 June. The warm front stretched southeastward from the low center across Iowa and into Illinois. Thunderstorms initially developed to the north and northeast of the low center by 1630 UTC 16 June in northern Nebraska and southern South Dakota, moving into western Minnesota by 2100 UTC. It was after the thunderstorms moved into Minnesota that the most violent tornadoes occurred.

The mesoscale model reproduces this general evolution of surface features but is slow in deepening the low and moving it to the northeast. At 0000 UTC 17 June the modeled low pressure center is located in central Nebraska, slightly over 300 km southwest of the observed location. This phase error is evident by 1800 UTC, suggesting that forecasters in real time would be able to make adjustments to their forecasts based upon the evolving differences between the model and observations. However, even though the model simulation is not perfect, an evaluation of the physically based severe weather parameters yields useful information. Values of CAPE indicate instability is present across much of the northern plains states by 1800 UTC (Fig. 6). A broad region of SREH values greater than $100 \text{ m}^2 \text{ s}^{-2}$, well within the range associated with the development of midlevel mesocyclones, also has developed. However, unlike the previous cases examined, the regions with values of BRNSHR between 40 and $100 \text{ m}^2 \text{ s}^{-2}$ are relatively small. The largest and most cohesive region of BRNSHR values within the approximate range associated with the development of low-level mesocyclones stretches across northern Nebraska and into Iowa, on the north side of the warm front, at 0000 UTC 27 April (Fig. 6b). Based upon the modeled values of BRNSHR and SREH found in southwestern Minnesota, we would initially expect nontornadic thunderstorms with strong outflows to be more likely where instead the violent tornadoes are reported. However, if the diagnosed model phase error is incorporated into our assessment by shifting these patterns a few hundred-kilometers to the northeast, then the region with observed tornadic supercell thunderstorms agrees well with the region having modeled BRNSHR values between 40

and $100 \text{ m}^2 \text{ s}^{-2}$ and SREH values greater than $200 \text{ m}^2 \text{ s}^{-2}$. These values suggest that supercell thunderstorms with low-level mesocyclones are likely.

It is curious that three of the four tornadic supercell thunderstorm outbreak cases have relatively broad, cohesive regions with BRNSHR values between 40 and $100 \text{ m}^2 \text{ s}^{-2}$ in the warm sector prior to or during convective development, while this 16 June case has only a limited region with higher BRNSHR values. This region of higher BRNSHR values occurs to the north and northeast of the low pressure center on the north side of the warm front and overlaps a region of larger SREH values as well. Part of this difference may be due to the model inaccurately reproducing the wind profile in low levels, as suggested by the differences between the observed and modeled values of BRNSHR (cf. Figs. 6b and 6c). However, Maddox et al. (1980) discuss the importance of thermal boundaries to the development of tornadic thunderstorms and indicate that thunderstorms interacting with a warm front or outflow boundary are likely to increase in severity and become tornadic. The model results presented here suggest that the reasons for this intensification may be that the wind profile is such that the balance between low-level baroclinic generation and outflow development is maintained in these regions, whereas the environments outside of the warm frontal zone are not conducive to this balance.

5. Synoptically evident outbreaks with bow echoes and widespread wind damage

The results from the above simulations suggest that the locations of model-produced convection and the distribution of CAPE can be used to help define areas where the potential exists for thunderstorms to develop, that SREH can be used to determine the likelihood of storm rotation, and that BRNSHR can be used to determine the likelihood of low-level mesocyclogenesis, or tornadoes. To determine whether or not this assessment has any utility for forecasting purposes, we now examine three synoptically-evident outbreak days in which bow echoes were the dominant convective storm type and most of the storm reports were of damaging straight-line winds. To fit our conceptual model, we would expect widespread damaging wind reports to occur in regions where the values of CAPE are positive, the values of SREH are larger than $100 \text{ m}^2 \text{ s}^{-2}$, and the values of BRNSHR are less than $40 \text{ m}^2 \text{ s}^{-2}$. The three cases chosen also are examined by Johns and Hart (1993).

a. 17 June 1992

Numerous tornadic supercells developed on 16 June 1992, but a change in the convective mode occurred after dark. By the morning of 17 June bow-echo-type storms with strong, damaging winds prevailed. Johns

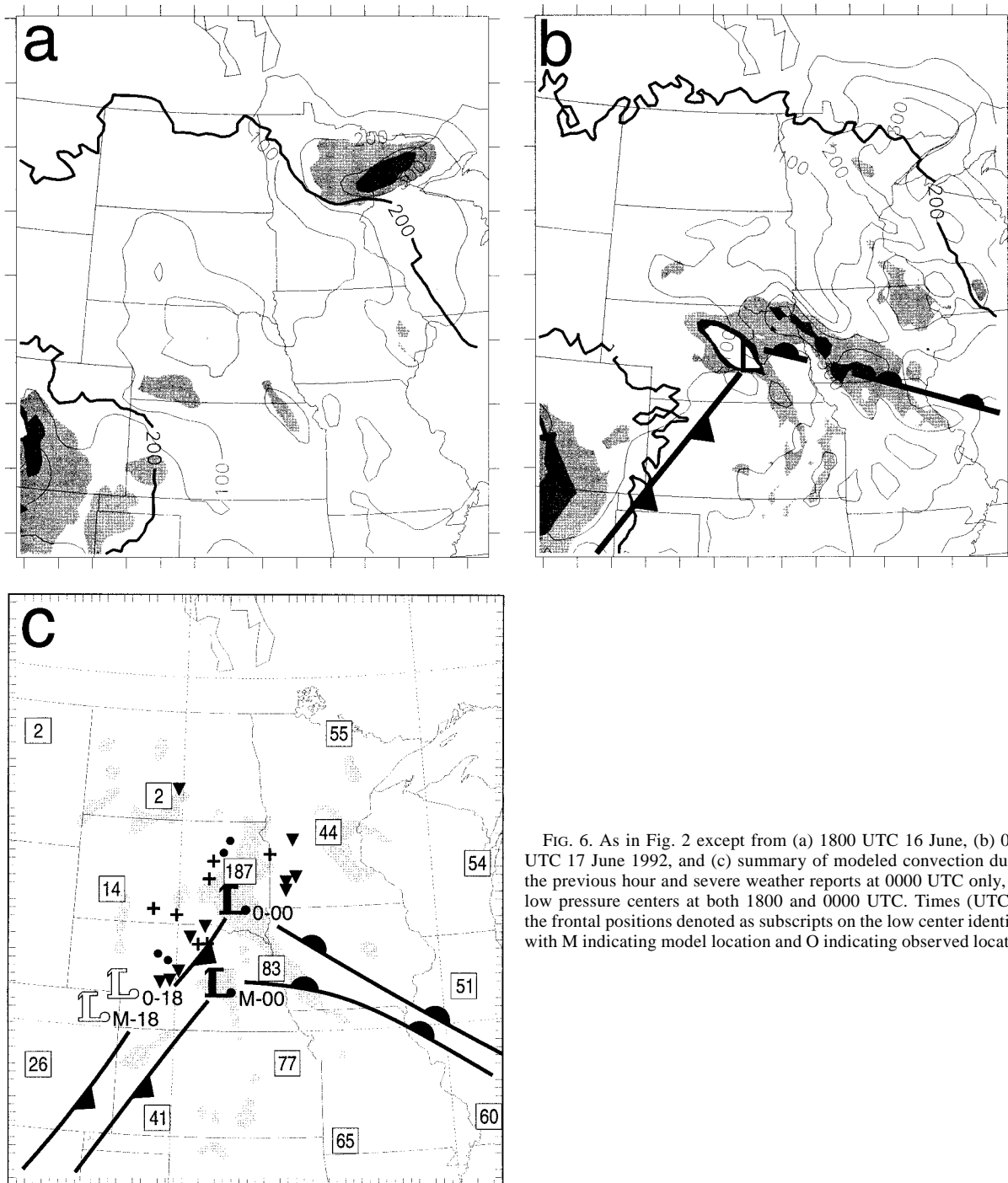


FIG. 6. As in Fig. 2 except from (a) 1800 UTC 16 June, (b) 0000 UTC 17 June 1992, and (c) summary of modeled convection during the previous hour and severe weather reports at 0000 UTC only, and low pressure centers at both 1800 and 0000 UTC. Times (UTC) of the frontal positions denoted as subscripts on the low center identifier, with M indicating model location and O indicating observed location.

and Hart (1993) indicate that there were 293 reports of damaging wind events, while only 29 tornadoes were reported. Of the tornado reports, only two were of F2 or greater severity. Thus, for each strong tornado report there were 147 reports of damaging winds. This is a dramatic difference from the tornadic supercell outbreak days examined previously.

At 1200 UTC 17 June convection already is active

from central Missouri northward into western Wisconsin. One of the two strong tornadoes is reported late in the morning in south-central Wisconsin. As the day progresses, the storms begin to organize, and by 0100 UTC 18 June a convective line stretches from eastern Michigan southwestward into southern Illinois. The development of convection produced by the mesoscale model roughly approximates these observations, although the

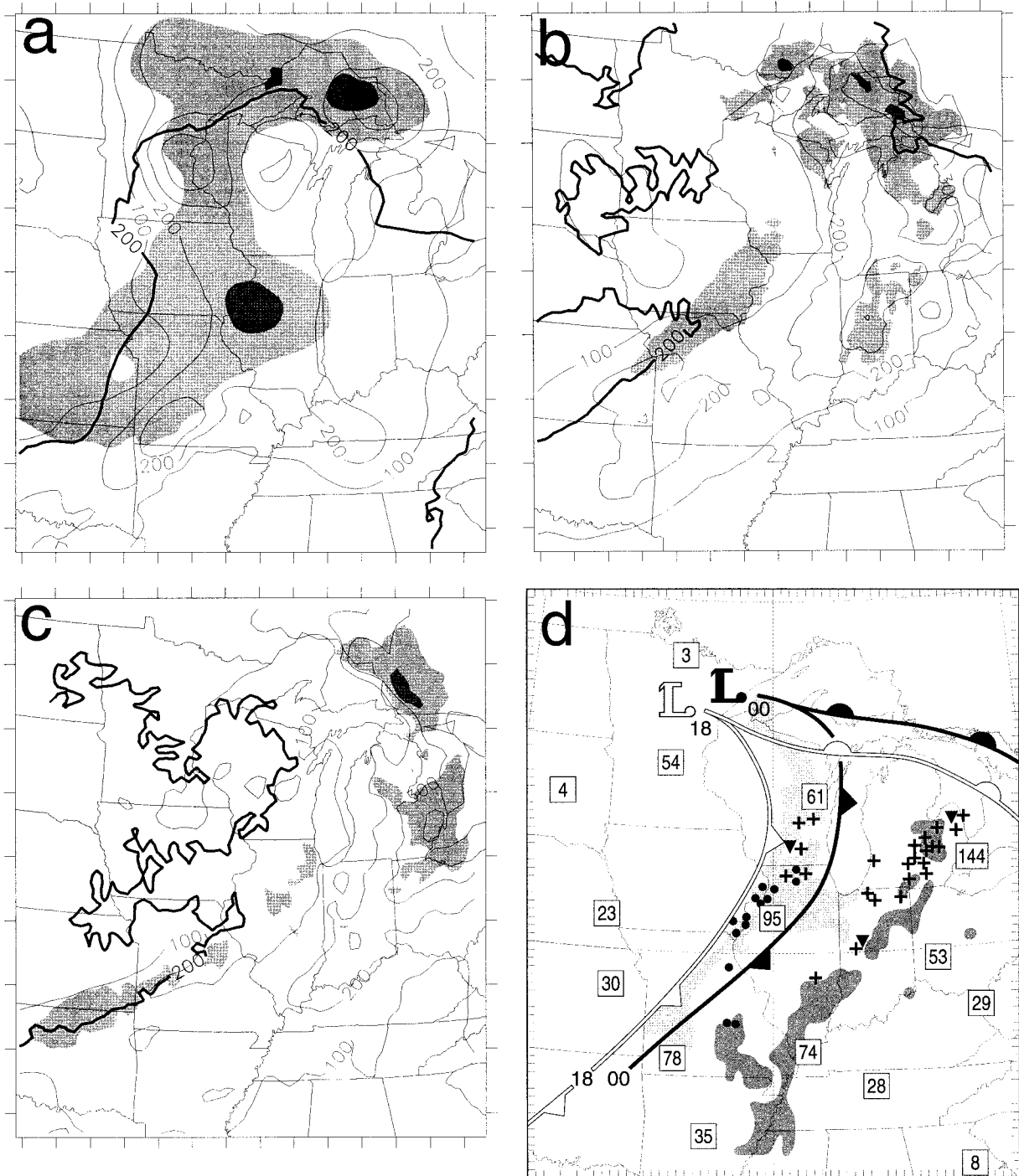


FIG. 7. As in Fig. 2 except from (a) 1200 UTC 17 June, (b) 1800 UTC 17 June, (c) 0000 UTC 18 June 1992, and (d) summary of modeled convection during the preceding hour and severe weather reports at both 1800 and 0000 UTC. (d) Reports from the hour preceding 1800 UTC are located in Wisconsin, Illinois, Iowa, and Missouri, with reports during the hour preceding 0000 UTC located elsewhere.

model convective line at 0100 UTC 18 June is not as well organized as that seen in the observations (not shown).

The evolution of the severe weather parameters on the morning of June 17 shows a transition is occurring.

There is a distinct decrease in the values of SREH and BRNSHR as the day progresses. Modeled values of CAPE at 1800 UTC (at the time of the one violent tornado in south-central Wisconsin) are positive throughout much of the midwest (Fig. 7b). Values of

SREH initially are above $200 \text{ m}^2 \text{ s}^{-2}$ across much of Wisconsin with a broad region of BRNSHR values above $40 \text{ m}^2 \text{ s}^{-2}$ (Fig. 7a). By 1800 UTC, the SREH values have decreased to below $100 \text{ m}^2 \text{ s}^{-2}$ across much of Wisconsin, while BRNSHR values have decreased to just slightly above $40 \text{ m}^2 \text{ s}^{-2}$ in a narrow zone stretching from northern Missouri into southwestern Wisconsin. Thus, with values of SREH below $100 \text{ m}^2 \text{ s}^{-2}$ it is impossible using our conceptual model to make any predictions of likely storm type in the environment throughout much of Wisconsin at this time. However, as discussed earlier, the effects of model-produced convection tend to diminish the values of SREH and BRNSHR such that earlier values of BRNSHR and SREH may be more representative of the preconvective environment. Values of BRNSHR and SREH at 1400 UTC (not shown) are supportive of low-level mesocyclogenesis occurring in Wisconsin. However, with the convection developing ahead of the frontal boundary it is clear that the storms are moving into an environment characterized by smaller values of BRNSHR. Indeed, damaging wind events dominate the severe weather reports later in the day.

By 0000 UTC 18 June, damaging winds are reported from northern Indiana into eastern Michigan, with one report of an F0 tornado in the thumb of Michigan and an F1 tornado in Indiana (Figs. 7c,d). Placement of modeled convective activity agrees reasonably well with the observations, indicating a general line of convection from Indiana to Michigan. Values of SREH within this region of modeled convection are above $200 \text{ m}^2 \text{ s}^{-2}$, and the values of BRNSHR are less than $40 \text{ m}^2 \text{ s}^{-2}$ over much of the Midwest with values of 10 to $20 \text{ m}^2 \text{ s}^{-2}$ over much of Indiana. Therefore, as the convective activity moved into an environment characterized by values of BRNSHR below $40 \text{ m}^2 \text{ s}^{-2}$ and SREH above $200 \text{ m}^2 \text{ s}^{-2}$, thunderstorms with strong outflows appear to dominate and damaging winds are the main severe weather threat. It is interesting that the weak tornado reported in Michigan occurred in a region with values of SREH greater than $300 \text{ m}^2 \text{ s}^{-2}$ and values of BRNSHR greater than $40 \text{ m}^2 \text{ s}^{-2}$, which the conceptual model indicates would be favorable for low-level mesocyclogenesis.

b. 9 April 1991

During the 24-h period beginning 1200 UTC 9 April 1991 there were 355 reports of damaging wind events and 22 reports of tornadoes, of which only two were determined to be F2 severity or greater. Thus, the ratio of the number of damaging wind reports to strong tornado reports is 178 (Johns and Hart 1993).

Thunderstorms are already developing in Arkansas at 1200 UTC 9 April along the cold front that stretches from eastern Texas northeastward through Arkansas, Missouri, and into Illinois. Over the next 12 h the cold front pushes slowly eastward into Tennessee, whereas

the convection organizes into several MCSs that move more rapidly eastward. At 0000 UTC at least three mesohighs are identifiable in the surface data and reports of thunderstorms stretch from Alabama northward to Pennsylvania.

The model simulation reproduces many of these features, including the development of convection at 1200 UTC in Arkansas and the rapid movement of convection eastward during the daytime. At 1800 UTC, there is a cluster of damaging wind reports in west-central Tennessee near where the model produced convection (Fig. 8). Values of SREH in this region are above $100 \text{ m}^2 \text{ s}^{-2}$, while BRNSHR values are typically between 10 and $50 \text{ m}^2 \text{ s}^{-2}$ in this zone of strong gradients in BRNSHR. This range of BRNSHR values could be used to support forecasts of either strong damaging winds or low-level mesocyclogenesis. However, by 0000 UTC the values of BRNSHR have decreased to below $40 \text{ m}^2 \text{ s}^{-2}$ across much of the warm sector. The main region of damaging winds at this time stretches from western North Carolina northward through West Virginia to Lake Erie, in agreement with the expectations from the conceptual model. It is notable that the SREH values are above $100 \text{ m}^2 \text{ s}^{-2}$ throughout this north-south corridor except in Virginia where there are no reports of wind damage. Therefore, this model-produced picture of convective storm type does yield useful guidance during much of this 12-h period, even though the model fails to produce parameterized convection in West Virginia.

c. 2 July 1992

The severe weather on this day begins over western Iowa near sunrise. During the 24-h period beginning 1200 UTC 2 July there are 266 reports of damaging winds and 14 reports of tornadoes, with only two tornadoes of F2 or greater severity (Johns and Hart 1993).

Thunderstorms initiate in eastern South Dakota near 0300 UTC 2 July behind the frontal boundary that stretches southwestward from southern Minnesota into western Kansas. These storms move into western Iowa 3 h later and become more organized as they march eastward across the state. By 1200 UTC the thunderstorms are in central and eastern Iowa. A well-defined mesohigh develops in eastern Iowa behind the intensifying convective line as seen by an examination of the surface data at 1800 UTC. After this time the convective activity moves rapidly eastward entering Indiana by 2100 UTC and Ohio by 0000 UTC 3 July (Fig. 9c).

The model simulation indicates a widespread region with positive CAPE at 1800 UTC with model-produced convection in northeastern Iowa and along the Minnesota-Wisconsin border, SREH values greater than $100 \text{ m}^2 \text{ s}^{-2}$ stretching in a zone from the Great Lakes into southern Illinois, and BRNSHR values less than $40 \text{ m}^2 \text{ s}^{-2}$ across much of the Midwest indicative of severe storms dominated by outflow (Fig. 9a). A region fa-

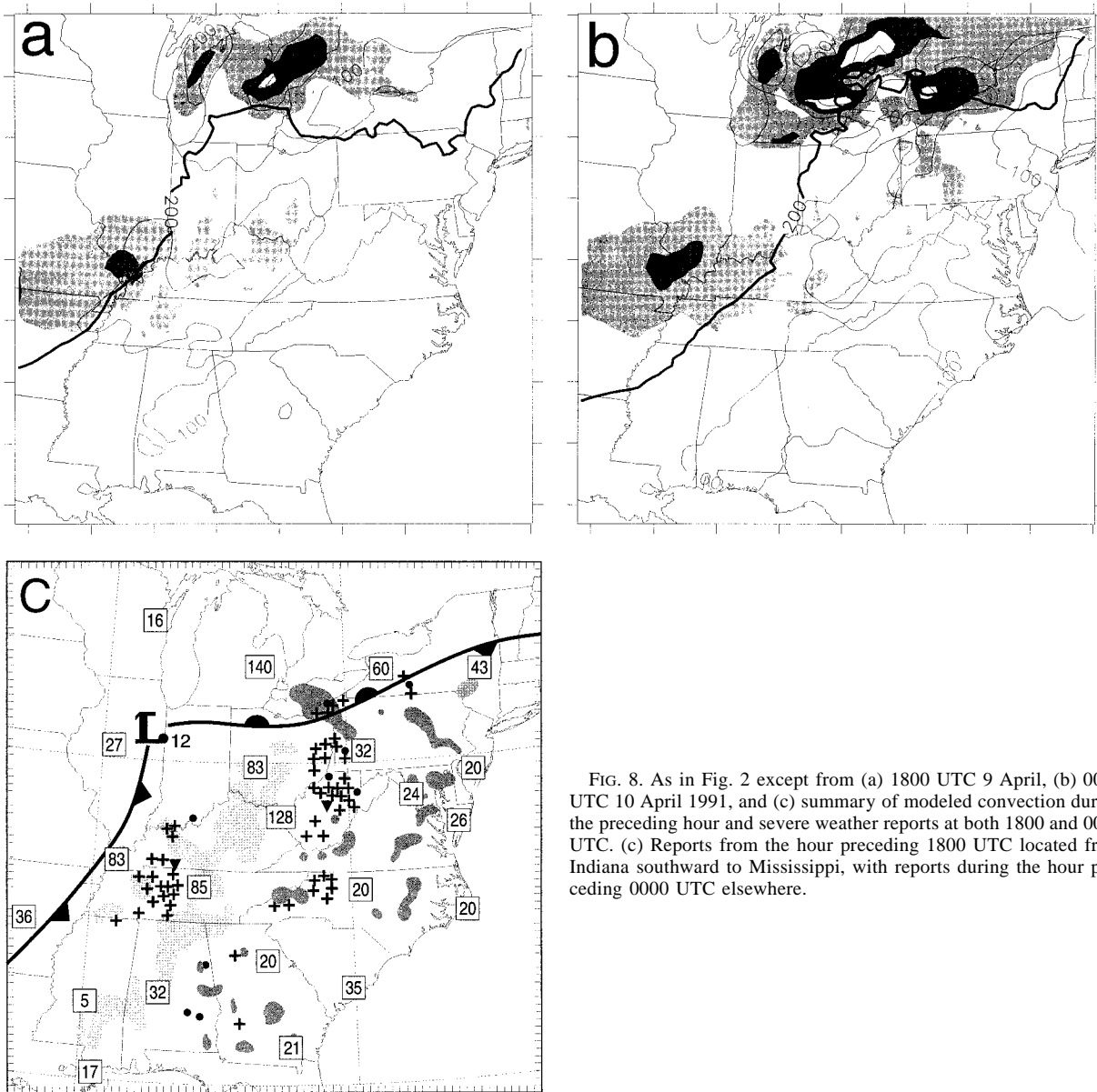


FIG. 8. As in Fig. 2 except from (a) 1800 UTC 9 April, (b) 0000 UTC 10 April 1991, and (c) summary of modeled convection during the preceding hour and severe weather reports at both 1800 and 0000 UTC. (c) Reports from the hour preceding 1800 UTC located from Indiana southward to Mississippi, with reports during the hour preceding 0000 UTC elsewhere.

avorable for tornadic supercells is centered in central Illinois where no convection occurs, and in western Wisconsin where thunderstorms develop, but there are no reports of severe weather. The main region of simulated convection is located along the Minnesota–Wisconsin border and in northeastern Iowa, in good correspondence with many of the locations of severe wind reports (Fig. 9c). Six hours later at 0000 UTC the tongue of higher SREH values has shifted eastward into western Indiana, while SREH values have increased to above $100 \text{ m}^2 \text{ s}^{-2}$ in Ohio (Fig. 9b). Values of BRNSHR remain between 5 and $20 \text{ m}^2 \text{ s}^{-2}$ across much of the Midwest south of the Great Lakes, while the modeled convective activity stretches east to west from Ohio into northern Missouri in good agreement with the severe wind reports

(Fig. 9c). An F3 tornado is on the ground in northeastern Oklahoma at 0000 UTC 3 July in a region where the model produces SREH values in excess of $100 \text{ m}^2 \text{ s}^{-2}$ but where the BRNSHR values still suggest thunderstorms dominated by outflow. This reinforces our statements that this technique should be used to define the dominant storm type only and should not be used to rule out the potential for other modes of convective activity.

6. Isolated severe thunderstorms with tornadic reports

Although the mesoscale model output appears to have utility in distinguishing between tornadic and

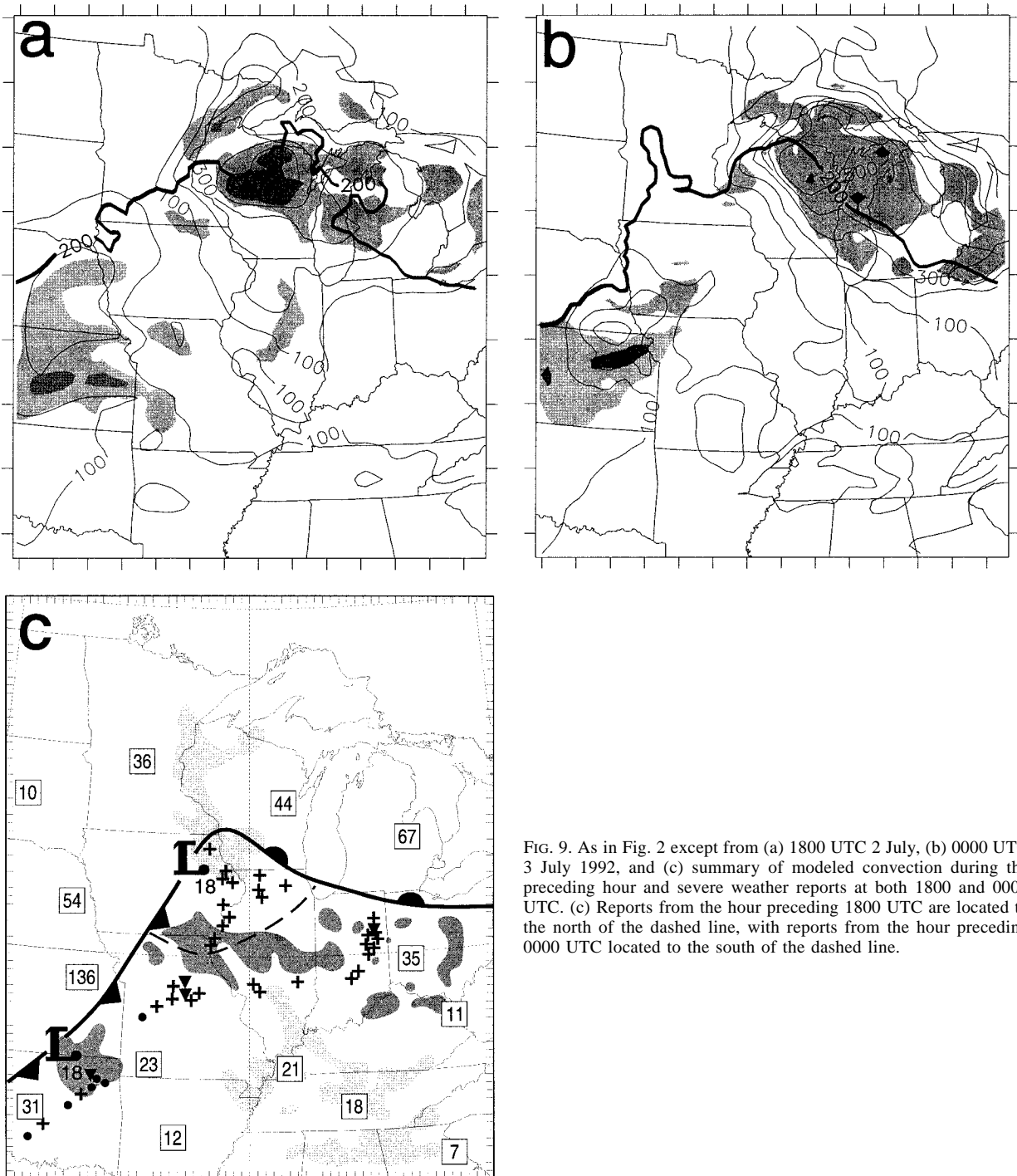


FIG. 9. As in Fig. 2 except from (a) 1800 UTC 2 July, (b) 0000 UTC 3 July 1992, and (c) summary of modeled convection during the preceding hour and severe weather reports at both 1800 and 0000 UTC. (c) Reports from the hour preceding 1800 UTC are located to the north of the dashed line, with reports from the hour preceding 0000 UTC located to the south of the dashed line.

outflow-dominated supercell thunderstorms on synoptically evident outbreak days, many life threatening events occur on a more local scale. To explore whether or not the parameter evaluation technique using values of SREH and BRNSHR has any value for isolated convective events, we choose two more cases to simulate.

a. 28 August 1990

On 28 August 1990 a climatologically rare and very destructive tornadic supercell developed in northern Illinois and moved through the towns of Plainfield and Crest Hill (NOAA 1991). This storm produced severe weather for over 4 h, making it unusually long lived as

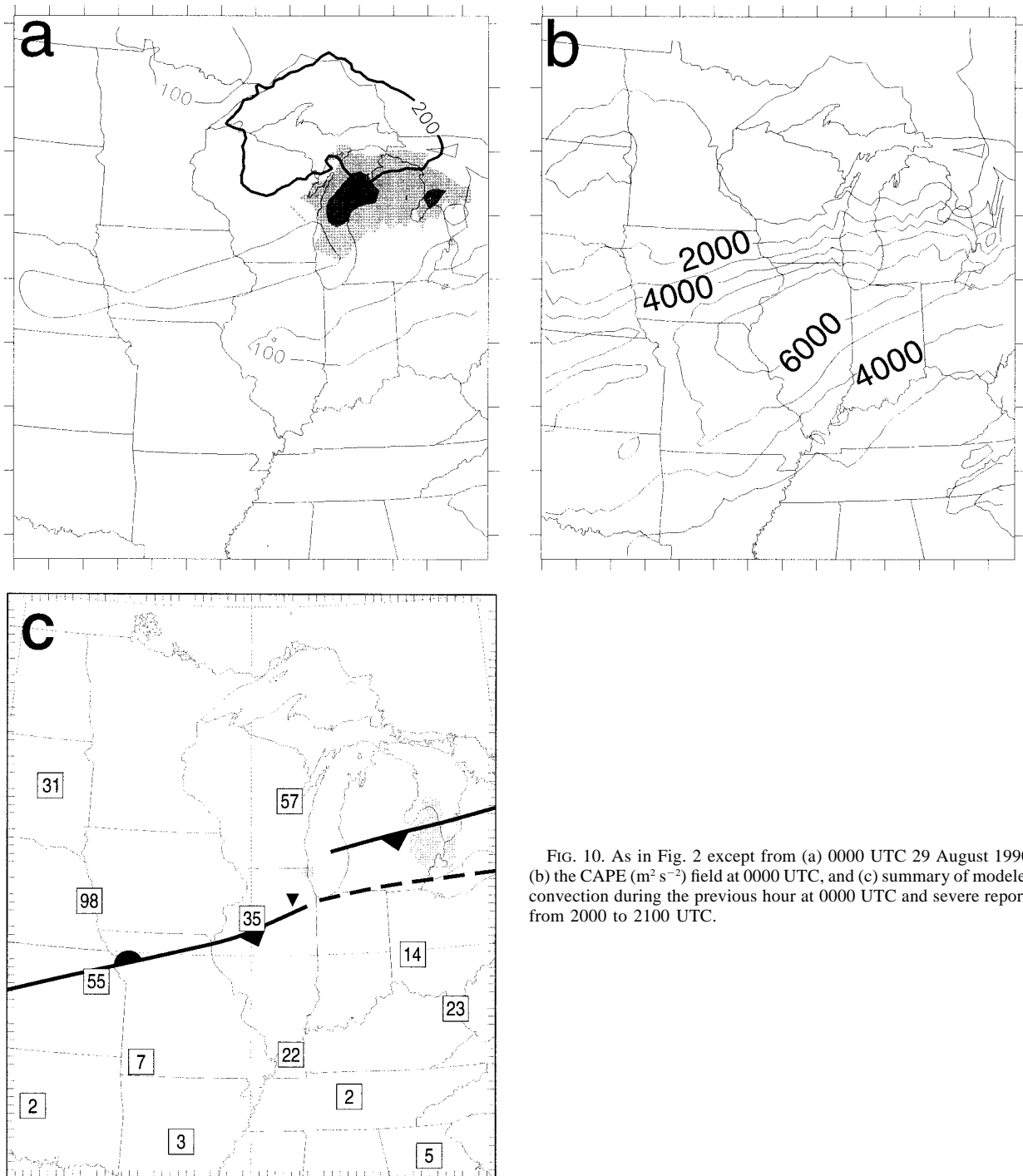


FIG. 10. As in Fig. 2 except from (a) 0000 UTC 29 August 1990, (b) the CAPE ($\text{m}^2 \text{s}^{-2}$) field at 0000 UTC, and (c) summary of modeled convection during the previous hour at 0000 UTC and severe reports from 2000 to 2100 UTC.

well. The thunderstorm initiated in northern Illinois just after 1800 UTC and slowly progressed southeastward during successive hours.

The mesoscale model simulation of this event does not produce any convection in Illinois until 0000 UTC when a small region of convection develops near Chicago (Fig. 10). Values of CAPE throughout Illinois are in excess of $4000 \text{ m}^2 \text{ s}^{-2}$ for most of the day. While the

SREH values at 1800 UTC are below $50 \text{ m}^2 \text{ s}^{-2}$ in northern Illinois, these values increase to above $100 \text{ m}^2 \text{ s}^{-2}$ across northern Illinois by 0000 UTC. Values of BRNSHR throughout the day are below $40 \text{ m}^2 \text{ s}^{-2}$ in northern Illinois, although a region of BRNSHR values greater than $40 \text{ m}^2 \text{ s}^{-2}$ is found over Lake Michigan by 0000 UTC 29 August 1990 when the model finally develops parameterized convection over Illinois. Observations

also suggest that BRNSHR values are greater to the north of the weak frontal boundary (Fig. 10c).

This evaluation suggests that the parameter evaluation techniques that show some ability to discriminate between tornadic and nontornadic days for synoptically evident outbreak events do not work well on this case. This may very well be due to limitations of the approach. But it is clear that the meteorological community does not know a great deal about thunderstorm evolution in very high CAPE environments. Therefore, we do not advocate using values of SREH and BRNSHR to evaluate the severe weather threat when the values of CAPE are much above $4000 \text{ m}^2 \text{ s}^{-2}$. We view any thunderstorms that develop in high CAPE environments to be potentially very dangerous (see Burgess and Lemon 1993) and believe our understanding of thunderstorms that form in high CAPE environments to be very limited.

b. 27 May 1985

At 1200 UTC 27 May 1985 a weak center of low pressure is located in the Texas panhandle close to the far northwestern corner of Oklahoma. Several decaying thunderstorms cover eastern Oklahoma, with one strong cell over the Red River in far northeastern Texas. The storms in eastern Oklahoma continue to weaken during the next few hours until by 1800 UTC the only active area of convection is the one thunderstorm in eastern Texas. However, at 1900 UTC a cell begins to develop along the dryline in far western Nebraska. Over the next 2 h this thunderstorm evolves into a tornadic supercell as it moves away from the dryline, producing a distinct hook echo as seen by radar and causing F3 damage across western Nebraska.

The mesoscale model simulation of this event fails to develop the initial convective activity in eastern Oklahoma at 1200 UTC. The model produces very little convection until 2000 UTC when the convective parameterization scheme is activated in western Nebraska, and by 0000 UTC 28 May the location of the model-produced convection agrees amazingly well with the location of the tornadic supercell in Nebraska (Fig. 11). Although this type of behavior cannot be expected in every mesoscale model simulation, it is encouraging to see that at times even isolated convective events can be reproduced reasonably well using a model with 25-km grid spacing.

The model fields of SREH initially highlight Oklahoma and central Kansas as having the potential for supercell thunderstorms (not shown). However, by 1800 UTC the region of positive CAPE values has been expanded outward, such that instability is now present in the front range of the Rocky Mountains. Values of SREH have increased dramatically along the high plains as upslope flow developed in the model simulation, producing favorable low-level wind shear with southeasterly flow in low levels veering to more westerly flow

aloft. By the time of the observed tornadic supercell, values of CAPE are above $1000 \text{ m}^2 \text{ s}^{-2}$ over western Nebraska, and values of SREH are greater than $100 \text{ m}^2 \text{ s}^{-2}$. Values of BRNSHR are above $40 \text{ m}^2 \text{ s}^{-2}$ in western Nebraska at 2100 UTC, at the time of convective initiation (not shown), suggesting that low-level mesocyclogenesis is possible and that this technique may be useful for some isolated convective events. However, these values decrease between 2100 and 0000 UTC in the area where convection begins, suggesting that it is important to examine these parameters prior to convection in order to minimize the influences of convection on these values. The model also produces convection in southeastern Colorado near a region favorable for low-level mesocyclogenesis. In this case, the model convective simulation is in error as no storms develop in this part of the state.

7. Summary

Nine severe weather events have been simulated using a mesoscale model, and the model data have been used to calculate several physically based parameters that have been shown to be related to the development of specific characteristics in thunderstorms. Johns and Hart (1993) have indicated that while the ability to forecast severe weather outbreaks in situations with strong forcing for upward motion is very good, it is difficult to distinguish between outbreak days that produce numerous tornadic supercell thunderstorms and those that produce bow echoes and widespread damaging winds. The differences in these two types of outbreaks are significant. For tornadic supercells the threats to the public are large but occur in spatially limited regions close to the track of the supercell. In contrast, for bow-echo-type storms the threat to the public is not quite as serious as with strong to violent tornadic supercells, but it occurs over very large regions.

In order to investigate our ability to discriminate between these two very different types of severe weather outbreaks, mesoscale model simulations of each type of event are produced. Four of the severe weather events simulated are tornadic supercell thunderstorm outbreaks that had numerous reports of strong to violent tornadoes. Three other of the severe weather events are bow-echo-type storms that had only a few strong tornadoes and a large number of damaging severe wind reports over a large region. Two other isolated tornadic supercell events are simulated to see if any of the results from the more strongly forced events are useful on isolated events as well.

Whereas a number of parameters have been used in the past to understand thunderstorm evolution, we focus primarily on three physically based parameters: CAPE, SREH, and BRNSHR. The values of CAPE highlight regions in which convection is possible, which can be further refined by examining other parameters, such as convective inhibition and model-pro-

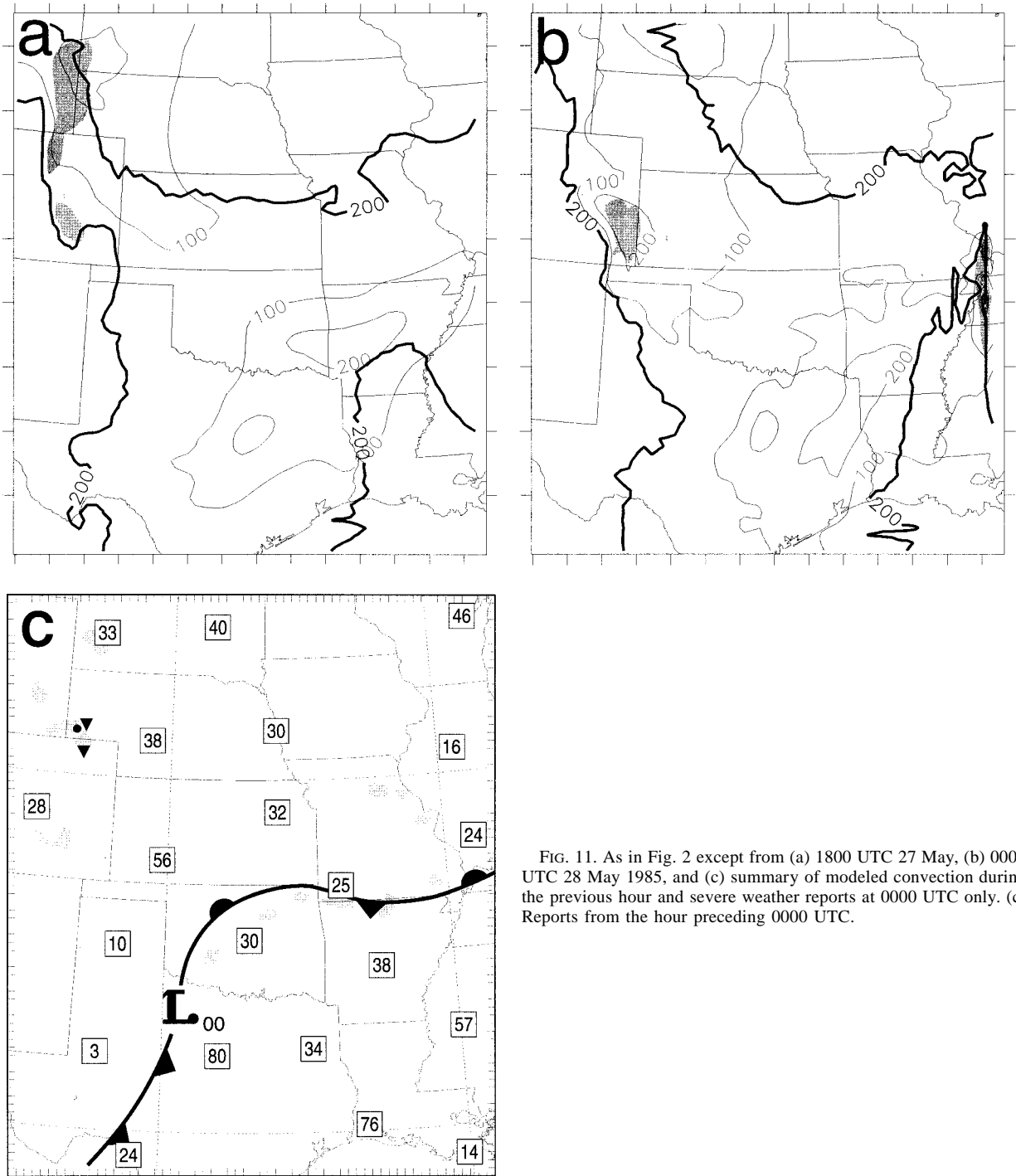


FIG. 11. As in Fig. 2 except from (a) 1800 UTC 27 May, (b) 0000 UTC 28 May 1985, and (c) summary of modeled convection during the previous hour and severe weather reports at 0000 UTC only. (c) Reports from the hour preceding 0000 UTC.

duced convective activity. Davies-Jones et al. (1990) and Droegemeier et al. (1993) indicate that SREH is a good indicator of the potential for thunderstorms to develop a midlevel mesocyclone. Thus, by examining CAPE, model-produced convective activity, and SREH, it is possible to develop a map of the regions where thunderstorms with strong midlevel mesocyclo-

nes, that is, supercells, may occur. Results from the mesoscale model simulations indicate that the model-produced fields of convective activity and SREH are very useful in determining regions where supercell thunderstorms are likely. Typically, supercell thunderstorms are reported in regions near where the model produces convection and values of SREH are greater

than $100 \text{ m}^2 \text{ s}^{-2}$. However these fields provide little guidance in determining if the supercells will become tornadic.

To attempt to discriminate between tornadic and nontornadic events, we apply the conceptual model of Brooks et al. (1994a,b). Their results, found using cloud-scale model simulations, suggest that the value of the storm-relative midlevel winds is an important factor in determining balance between baroclinic generation of vorticity in low levels, owing to the evaporation of rain, and outflow development. Since the development of low-level mesocyclones is related to the baroclinic generation of positive vertical vorticity, the evolution of the storm outflow is very important to consider. We have found that the values of BRNSHR can be used as a proxy for the storm-relative midlevel winds. Results from the mesoscale model simulations suggest that values of BRNSHR below $40 \text{ m}^2 \text{ s}^{-2}$ or so are associated with storms that are outflow dominated, while values of BRNSHR between 40 and $100 \text{ m}^2 \text{ s}^{-2}$ or so are associated with storms that produce low-level mesocyclones. Thus, regions where the potential for tornadic supercell thunderstorms exists may be identified by looking for values of positive CAPE near regions of model-produced convective activity, values of SREH greater than $100 \text{ m}^2 \text{ s}^{-2}$, and values of BRNSHR greater than 40 and less than $100 \text{ m}^2 \text{ s}^{-2}$. As the BRNSHR values increase, the values of SREH also must increase in order to increase the likelihood of low-level mesocyclogenesis. In contrast, regions where the potential for bow echoes and damaging straight-line winds exists may be identified by looking for values of SREH greater than $100 \text{ m}^2 \text{ s}^{-2}$ and values of BRNSHR less than $40 \text{ m}^2 \text{ s}^{-2}$. Therefore, a careful examination of these three parameters makes it possible to discriminate between thunderstorms that are more likely to develop low-level mesocyclones and those that are not on many days.

Although these results are very encouraging, we have examined only nine cases. In one of these cases, the 28 August 1990 isolated tornadic supercell event in Illinois, the parameters did not fall within the ranges described above for our conceptual model. Thus, it is important that this approach be viewed as just another tool in the arsenal of the forecaster. It is by no means the last word in trying to identify regions of potential tornadic supercell thunderstorm development. Indeed, the results of Brooks et al. (1994a, b) only apply to rotating thunderstorms, such that tornadoes that form in environments with low values of SREH may not be identified using the technique outlined in this paper. While the results discussed herein suggest that improvements in the identification of tornadic supercell environments can be made, we hope that future research will provide even better methods for discriminating between tornadic and nontornadic thunderstorms.

Acknowledgments. We greatly appreciate reviews of earlier versions of this manuscript by Chuck Doswell,

Mike Branick, and two anonymous reviewers, whose comments strengthened our presentation. Daniel V. Mitchell provided computer graphics support, while Joan O'Bannon drafted many of the figures. Their assistance is greatly appreciated. Steve Hankin and Jerry Davison of the NOAA Pacific Marine Environmental Laboratory are gratefully acknowledged for the development and free dissemination of FERRET, an interactive display package that was used to assist in the examination of the model data. The PSU-NCAR modeling system is maintained through the efforts of many scientists at both the Pennsylvania State University and NCAR/MMM and we are grateful for all their hard work and dedication to making this model easily accessible and user friendly. Data for initializing the model came from the Scientific Computing Division of NCAR.

REFERENCES

- Anthes, R. A., and T. T. Warner, 1978: Development of hydrodynamic models suitable for air pollution and other mesometeorological studies. *Mon. Wea. Rev.*, **106**, 1045–1078.
- , E.-Y. Hsie, and Y.-F. Li, 1987: Description of the Penn State/NCAR Mesoscale Model Version 4 (MM4). NCAR Tech. Note NCAR/TN-282+STR, 66 pp. [Available from NCAR, P.O. Box 3000, Boulder, CO 80307.]
- Benjamin, S. G., 1983: Some effects of heating and topography on the regional severe storm environment. Ph.D. thesis, The Pennsylvania State University, University Park, PA, 265 pp. [Available from University Microfilm, 300 N. Zeeb Rd., P.O. Box 1346, Ann Arbor, MI 46801-1346.]
- , and N. L. Seaman, 1985: A simple scheme for improved objective analysis in curved flow. *Mon. Wea. Rev.*, **113**, 1184–1198.
- Black, T. L., 1994: The new NMC mesoscale eta model: Description and forecast examples. *Wea. Forecasting*, **9**, 265–278.
- Blackadar, A. K., 1976: Modeling the nocturnal boundary layer. Preprints, *Third Symp. on Atmospheric Turbulence, Diffusion, and Air Quality*, Raleigh, NC, Amer. Meteor. Soc., 46–49.
- , 1979: High resolution models of the planetary boundary layer. *Advances in Environmental Science and Engineering*, Vol. 1, No. 1, J. Pfafflin and E. Ziegler, Eds., Gordon and Breach, 50–85.
- Brooks, H. E., C. A. Doswell III, and R. B. Wilhelmson, 1994a: On the role of midtropospheric winds in the evolution and maintenance of low-level mesocyclones. *Mon. Wea. Rev.*, **122**, 126–136.
- , —, and J. Cooper, 1994b: On the environments of tornadic and nontornadic mesocyclones. *Wea. Forecasting*, **9**, 606–618.
- Burgess, D. W., and L. R. Lemon, 1993: Tornado and mesocyclone development in a low-shear environment: The Cashion, Oklahoma storm of June 18, 1992. Preprints, *17th Conf. on Severe Local Storms*, Saint Louis, MO, Amer. Meteor. Soc., 153–157.
- Colman, B. R., and C. F. Mass, 1996: Real-time mesoscale modeling in the Pacific Northwest. Preprints, *15th Conf. on Weather Analysis and Forecasting*, Norfolk, VA, Amer. Meteor. Soc., 191–192.
- Cortinas, J. V., Jr., and D. J. Stensrud, 1995: The importance of understanding mesoscale model parameterization schemes for weather forecasting. *Wea. Forecasting*, **10**, 716–740.
- Davies, J., and R. Johns, 1993: Some wind and instability parameters associated with strong and violent tornadoes. Part I: Wind shear and helicity. *The Tornado: Its Structure, Dynamics, Prediction and Hazards, Geophys. Monogr.*, No. 79, Amer. Geophys. Union, 573–582.
- Davies-Jones, R., D. Burgess, and M. Foster, 1990: Test of helicity as a tornado forecast parameter. Preprints, *16th Conf. Severe Local Storms*, Kananaskis Park, AB, Canada, Amer. Meteor. Soc., 588–592.
- Doswell, C., III, 1987: The distinction between large-scale and me-

- mesoscale contribution to severe convection: A case study example. *Wea. Forecasting*, **2**, 3–16.
- Droegemeier, K. K., S. M. Lazarus, and R. Davies-Jones, 1993: The influence of helicity on numerically simulated convective storms. *Mon. Wea. Rev.*, **121**, 2005–2029.
- Fritsch, J. M., and C. F. Chappell, 1980: Numerical prediction of convectively driven mesoscale pressure systems. Part I: Convective parameterization. *J. Atmos. Sci.*, **37**, 1722–1733.
- Fujita, T. T., and D. Steigler, 1985: Detailed analysis of the tornado outbreak in the Carolinas. Preprints, *14th Conf. on Severe Local Storms*, Indianapolis, IN, Amer. Meteor. Soc., 271–274.
- Gyakum, J. R., and E. S. Barker, 1988: A case study of explosive subsynoptic-scale cyclogenesis. *Mon. Wea. Rev.*, **116**, 2225–2253.
- Hsie, E.-Y., R. A. Anthes, and D. Keyser, 1984: Numerical simulation of frontogenesis in a moist atmosphere. *J. Atmos. Sci.*, **41**, 2581–2594.
- Johns, R., and C. Doswell III, 1992: Severe local storms forecasting. *Wea. Forecasting*, **7**, 588–612.
- , and J. A. Hart, 1993: Differentiating between types of severe thunderstorm outbreaks: A preliminary investigation. Preprints, *17th Conf. on Severe Local Storms*, Saint Louis, MO, Amer. Meteor. Soc., 46–50.
- , J. Davies, and P. Leftwich, 1993: Some wind and instability parameters associated with strong and violent tornadoes. Part II: Variations in the combinations of wind and instability parameters. *The Tornado: Its Structure, Dynamics, Prediction and Hazards, Geophys. Monogr.*, No. 79, Amer. Geophys. Union, 583–590.
- July, M. J., and R. H. John, 1993: Assessment of “high risk” forecasts issued by the National Severe Storms Forecast Center in the 0700 UTC day-one convective outlook. Preprints, *17th Conf. on Severe Local Storms*, Saint Louis, MO, Amer. Meteor. Soc., 133–137.
- Kain, J. S., and J. M. Fritsch, 1990: A one-dimensional entraining/detraining plume model and its application in convective parameterization. *J. Atmos. Sci.*, **47**, 2784–2802.
- , and —, 1992: The role of the convective “trigger function” in numerical forecasts of mesoscale convective systems. *Meteor. Atmos. Phys.*, **49**, 93–106.
- Korotky, W., R. W. Przybylinski, and J. A. Hart, 1993: The Plainfield, Illinois, tornado of August 28, 1990: The evolution of synoptic and mesoscale environments. *The Tornado: Its Structure, Dynamics, Prediction and Hazards, Geophys. Monogr.*, No. 79, Amer. Geophys. Union, 611–624.
- Lazarus, S. M., and K. K. Droegemeier, 1990: The influence of helicity on the stability and morphology of numerically simulated storms. Preprints, *16th Conf. on Severe Local Storms*, Kananaskis Park, AB, Canada, Amer. Meteor. Soc., 269–274.
- Lin, Y.-L., R. D. Farley, and H. D. Orville, 1983: Bulk parameterization of the snow field in a cloud model. *J. Climate Appl. Meteor.*, **22**, 1065–1092.
- Maddox, R. A., L. R. Hoxit, and C. F. Chappell, 1980: A study of tornadic thunderstorm interactions with thermal boundaries. *Mon. Wea. Rev.*, **108**, 322–336.
- McPherson, R. D., 1994: The National Centers for Environmental Prediction: Operational climate, ocean, and weather prediction for the 21st century. *Bull. Amer. Meteor. Soc.*, **75**, 363–373.
- Miller, R., 1972: Notes on analysis and severe-storm forecasting procedures of the Air Force Global Weather Center. Air Weather Service Tech. Rep. 200 (Rev.), Air Weather Service, Scott Air Force Base, IL, 190 pp. [Available from Air Weather Service, Technical Library, 859 Buchanan St., Scott AFB, IL 62225-5118.]
- Molinari, J., and M. Dudek, 1992: Parameterization of convective precipitation in mesoscale models: A critical review. *Mon. Wea. Rev.*, **120**, 326–344.
- Moller, A. R., C. A. Doswell III, M. P. Foster, and G. R. Woodall, 1994: The operational recognition of supercell thunderstorm environments and storm structures. *Wea. Forecasting*, **9**, 327–347.
- Moncrieff, M. W., and J. S. A. Green, 1972: The propagation and transfer properties of steady convective overturning in shear. *Quart. J. Roy. Meteor. Soc.*, **98**, 336–352.
- NOAA, 1991: Natural Disaster Survey Report: The Plainfield/Crest Hill tornado. U.S. Dept. of Commerce, National Weather Service, Silver Spring, MD, 43 pp. [Available from National Weather Service Headquarters, Silver Spring, MD 20910.]
- Rutledge, S. A., and P. V. Hobbs, 1983: The mesoscale and microscale structure and organization of clouds and precipitation in midlatitude cyclones. VIII: A model for the “seeder-feeder” process in warm-frontal rainbands. *J. Atmos. Sci.*, **40**, 1185–1206.
- Steenburgh, W. J., and D. J. Onton, 1996: An evaluation of a real-time mesoscale prediction system based on the Penn State/NCAR mesoscale model. Preprints, *15th Conf. on Weather Analysis and Forecasting*, Norfolk, VA, Amer. Meteor. Soc., 183–186.
- Stensrud, D. J., and J. M. Fritsch, 1994: Mesoscale convective systems in weakly forced large-scale environments. Part III: Numerical simulations and implications for operational forecasting. *Mon. Wea. Rev.*, **122**, 2084–2104.
- Weisman, M. L., 1993: The genesis of severe, long-lived bow echoes. *J. Atmos. Sci.*, **50**, 645–670.
- , and J. B. Klemp, 1982: The dependence of numerically simulated convective storms on vertical wind shear and buoyancy. *Mon. Wea. Rev.*, **110**, 504–520.
- , and —, 1984: The structure and classification of numerically simulated convective storms in directionally varying wind shear. *Mon. Wea. Rev.*, **112**, 2479–2498.
- Zhang, D.-L., 1989: The effect of parameterized ice microphysics on the simulation of vortex circulation with a mesoscale hydrostatic model. *Tellus*, **41A**, 132–147.
- , and R. A. Anthes, 1982: A high-resolution model of the planetary boundary layer—Sensitivity tests and comparisons with SESA-ME-79 data. *J. Appl. Meteor.*, **21**, 1594–1609.
- , and J. M. Fritsch, 1986: Numerical simulation of the meso- β scale structure and evolution of the 1977 Johnstown flood. Part I: Model description and verification. *J. Atmos. Sci.*, **43**, 1913–1943.
- , H.-R. Chang, N. L. Seaman, T. T. Warner, and J. M. Fritsch, 1986: A two-way interactive nesting procedure with variable terrain resolution. *Mon. Wea. Rev.*, **114**, 1330–1339.
- , K. Gao, and D. B. Parsons, 1989: Numerical simulation of an intense, squall line during 10–11 June 1985 PRE-STORM. Part I: Model verification. *Mon. Wea. Rev.*, **117**, 960–994.
- Zheng, Y., Q. Xu, and D. J. Stensrud, 1995: A numerical study of the 7 May 1985 mesoscale convective system. *Mon. Wea. Rev.*, **123**, 1781–1799.